RESEARCH ARTICLE
Molecular Biology and Physiology

(p)ppGpp/GTP and Malonyl-CoA Modulate *Staphylococcus aureus* Adaptation to FASII Antibiotics and Provide a Basis for Synergistic Bi-Therapy

Amit Pathania,[a] Jamila Anba-Mondoloni,[a] Myriam Gominet,[b] David Halpern,[a] Julien Dairou,[c] Laëtitia Dupont,[a] Gilles Lamberet,[a] Patrick Trieu-Cuot,[b] Karine Gloux,[a] Alexandra Gruss[a]

[a]Micalis Institute, INRAE, AgroParisTech, Université Paris-Saclay, Jouy en Josas, France
[b]Unité de Biologie des Pathogènes à Gram-positif, CNRS UMR 2001, Institut Pasteur, Paris, France
[c]Université de Paris, CNRS UMR8601, Paris, France

ABSTRACT Fatty acid biosynthesis (FASII) enzymes are considered valid targets for antimicrobial drug development against the human pathogen *Staphylococcus aureus*. However, incorporation of host fatty acids confers FASII antibiotic adaptation that compromises prospective treatments. *S. aureus* adapts to FASII inhibitors by first entering a nonreplicative latency period, followed by outgrowth. Here, we used transcriptional fusions and direct metabolite measurements to investigate the factors that dictate the duration of latency prior to outgrowth. We show that stringent response induction leads to repression of FASII and phospholipid synthesis genes. (p)ppGpp induction inhibits synthesis of malonyl-CoA, a molecule that derepresses FapR, a key regulator of FASII and phospholipid synthesis. Anti-FASII treatment also triggers transient expression of (p)ppGpp-regulated genes during the anti-FASII latency phase, with concomitant repression of FapR regulon expression. These effects are reversed upon outgrowth. GTP depletion, a known consequence of the stringent response, also occurs during FASII latency, and is proposed as the common signal linking these responses. We next showed that anti-FASII treatment shifts malonyl-CoA distribution between its interactants FapR and FabD, toward FapR, increasing expression of the phospholipid synthesis genes *plsX* and *plsC* during outgrowth. We conclude that components of the stringent response dictate malonyl-CoA availability in *S. aureus* FASII regulation, and contribute to latency prior to anti-FASII-adapted outgrowth. A combinatory approach, coupling a (p)ppGpp inducer and an anti-FASII, blocks *S. aureus* outgrowth, opening perspectives for bi-therapy treatment.

IMPORTANCE *Staphylococcus aureus* is a major human bacterial pathogen for which new inhibitors are urgently needed. Antibiotic development has centered on the fatty acid synthesis (FASII) pathway, which provides the building blocks for bacterial membrane phospholipids. However, *S. aureus* overcomes FASII inhibition and adapts to anti-FASII by using exogenous fatty acids that are abundant in host environments. This adaptation mechanism comprises a transient latency period followed by bacterial outgrowth. Here, we use metabolite sensors and promoter reporters to show that responses to stringent conditions and to FASII inhibition intersect, in that both involve GTP and malonyl-CoA. These two signaling molecules contribute to modulating the duration of latency prior to *S. aureus* adaptation outgrowth. We exploit these novel findings to propose a bi-therapy treatment against staphylococcal infections.

KEYWORDS anti-FASII adaptation, (p)ppGpp, GTP, malonyl-CoA, phospholipids, antibiotic bi-therapy, triclosan, mupirocin, CodY

Citation Pathania A, Anba-Mondoloni J, Gominet M, Halpern D, Dairou J, Dupont L, Lamberet G, Trieu-Cuot P, Gloux K, Gruss A. 2021. (p)ppGpp/GTP and malonyl-CoA modulate *Staphylococcus aureus* adaptation to FASII antibiotics and provide a basis for synergistic bi-therapy. mBio 12:e03193-20. https://doi.org/10.1128/mBio.03193-20.

Editor Indranil Biswas, KUMC

Address correspondence to Amit Pathania, amit.pathania@inrae.fr, or Alexandra Gruss, alexandra.gruss@inrae.fr.

Received 22 November 2020
Accepted 3 December 2020
Published 2 February 2021

Bacterial infections that fail to respond to antibiotic treatments are on the rise, especially in the immunocompromised or weakened host, underlining the need for novel antimicrobial strategies (1). The fatty acid synthesis (FASII) enzymes were considered fail-safe targets for eliminating numerous Gram-positive pathogens. Anti-FASII drugs have been a front-line treatment against *Mycobacterium tuberculosis*, which synthesizes very long-chain fatty acids that cannot be compensated by the host (2). However, *Firmicute* pathogens, including *Staphylococcus aureus* and numerous members of the *Streptococcaceae*, bypass FASII inhibition and satisfy their fatty acid requirements by using host-supplied fatty acids (3–5). FASII inhibitors, such as triclosan (Tric), MUT056399, fasamycins A and B, amycomicin, and a pipeline FASII antibiotic AFN-1252 (6–11), would thus have limited use as stand-alone treatments of infections by numerous Gram-positive pathogens (3–5).

Our recent studies show that *S. aureus* can adapt to FASII inhibitors by two mechanisms, depending on growth conditions. One involves mutations in a FASII initiation gene, usually *fabD*. Lower activity of the FabD mutant would increase availability of its substrates, one of which is acyl carrier protein (ACP), for incorporation of exogenous fatty acids (eFA) via the phosphate acyltransferase PlsX (Fig. S1A in the supplemental material) (4, 12). The second mode of adaptation occurs without FASII mutations and predominates in serum-supplemented medium. In this case, full adaptation and eFA incorporation in actively growing cells is achieved after a latency phase, whose duration (6 to 12 h) depends on the strain and pregrowth in serum-containing medium. Adaptation is associated with greater intracellular retention of eFA and ACP, both of which contribute to eFA incorporation in membrane phospholipids to compensate FASII inhibition (Fig. S1B) (5).

The factors regulating *S. aureus* transition from latency to outgrowth upon anti-FASII treatment remain unknown. We hypothesized that initial fatty acid starvation in response to anti-FASII might comprise the signal that delays eFA incorporation in phospholipids and outgrowth. The *S. aureus* FapR repressor reportedly regulates most FASII genes (except *acc*, encoding acetyl-CoA carboxylase, and FabZ, β-hydroxyacyl-ACP dehydratase) together with phospholipid synthesis genes *plsX* and *plsC* (13, 14). Interestingly, malonyl-CoA has a dual function; it is the first dedicated FASII substrate used by FabD (malonyl-CoA transacylase), and it also controls FapR by a feed-forward mechanism (14). FabD uses malonyl-CoA and ACP to synthesize malonyl-ACP (15). Malonyl-CoA binding to FapR reverses FapR repression, leading to upregulation of the FASII and phospholipid synthesis genes (14). Thus, malonyl-CoA is important in both enzymatic and regulatory activities of FASII. In *Escherichia coli*, expression of the malonyl-CoA synthesis enzyme ACC is regulated by (p)ppGpp, which accumulates in slow growing, nutrient-deficient conditions (16, 17); (p)ppGpp also reportedly regulates other FASII and phospholipid synthesis genes (18, 19). In *Bacillus subtilis*, studies of (p)ppGpp null mutants gave evidence for the need to activate the stringent response in order to survive fatty acid starvation; these studies implicated increased GTP in mortality of (p)ppGpp null mutant strains (20). Fatty acid starvation is also associated with cell size via regulation of FASII, although underlying mechanisms remain to be elucidated (21). To our knowledge, no evidence exists for stringent response-mediated FASII regulation in *S. aureus*.

Here, we first show that stringent response induction exerts control over fatty acid and phospholipid synthesis in *S. aureus* by modulating FapR repressor activity. FASII antibiotic treatment, like the stringent response, leads to GTP depletion, which is the likely common metabolite linking these two responses. The chain of events revealed here indicate that (p)ppGpp/GTP and malonyl-CoA contribute to adjusting the timing of FASII-antibiotic-induced latency transition to outgrowth. Based on our findings, we suggest a bi-therapy approach that combines FASII inhibitors and a (p)ppGpp inducer to prevent *S. aureus* adaptation.

RESULTS

(p)ppGpp negatively regulates malonyl-CoA levels in *S. aureus*. We investigated the potential roles of (p)ppGpp and malonyl-CoA in *S. aureus* response to FASII

inhibition. Three *S. aureus* strains were used in this study, Newman, USA300, and HG1-R (Table S1), which all adapt to anti-FASII with similar kinetics (5, this study). Previous studies reported difficulties in (p)ppGpp measurements in *B. subtilis* and *S. aureus* (20, 22). Our initial attempts at measuring (p)ppGpp by high-pressure liquid chromatography (HPLC) and the fluorescent dye PyDPA (23) failed to give reliable results (data not shown). We therefore constructed transcriptional fusions to detect conditions when (p)ppGpp-induced genes are activated *in vivo* (Table S2). The reporter fusion activities responded to mupirocin, which inhibits isoleucyl-tRNA synthetase and triggers (p)ppGpp synthesis (24) (Fig. 1A and data not shown). P_{ilvD}-*lacZ* (NWMN_1960) and P_{oppB}-*lacZ* (NWMN_0856) were upregulated, and P_{cshA}-*lacZ* (NWMN_1985) was downregulated by mupirocin. Nutrient starvation during stationary phase induces the stringent response in *E. coli* (16). In *S. aureus*, β-galactosidase (β-gal) activity of the P_{ilvD}-*lacZ* and P_{oppB}-*lacZ* sensors were 1.2- and 7-fold higher in stationary phase compared to exponential-phase cells, while P_{cshA}-*lacZ* activity was ~2-fold lower (Fig. 1B and data not shown), further validating the *in vivo* (p)ppGpp sensors.

The stringent response sensors would be expected not to respond to mupirocin in a (p)ppGpp null strain. We compared sensor responses in (p)ppGpp-proficient and deficient strains. These strains derive from HG001 (25) and a (p)ppGpp-null strain (kindly provided by C. Wolz) (26). They were first repaired for a defect in *fakB1*, which is common to 8325 derivatives (like HG001) and a minority of *S. aureus* isolates (5). FakB1, a fatty acid kinase subunit, facilitates assimilation of mainly saturated fatty acids (27). Its absence in 8325 derivatives can explain previous reports of *S. aureus* sensitivity to anti-FASII treatment (11, 28), although the majority of *S. aureus* strains adapt to these antibiotics (4, 5). The *fakB1*-repaired HG001 and HG001 (p)ppGpp0 strains are referred to respectively as HG1-R and ppGpp0. Responses of the P_{ilvD}-*lacZ*, and P_{cshA}-*lacZ* reporter fusions were compared in HG1-R and ppGpp0 strains by plate tests (Fig.S2; see Materials and Methods). If the response to mupirocin occurs via its stimulation of (p)ppGpp, then neither induction of *ilvD* nor suppression of *cshA* would occur in the ppGpp0 background. Indeed, P_{ilvD}-*lacZ* (Fig. S2A) and P_{cshA}-*lacZ* (Fig. S2B) responded to mupirocin as expected in the parental strain, whereas no such responses were observed in the ppGpp0 background. These results also indicate that the stringent response controls these sensors in *S. aureus*.

We then asked whether (p)ppGpp blocks malonyl-CoA synthesis in *S. aureus*, as reported in *E. coli* (29), despite major regulatory differences between these bacteria. Total malonyl-CoA was measured in cells treated or not with mupirocin by enzyme-linked immunosorbent assay (ELISA). We also used the *in vivo* promoter fusion P_{accBC}-*lacZ* to measure expression of *accBC* (NWMN_1432 and NWMN_1431), which encode subunits of acetyl-CoA carboxylase (ACC) required for malonyl-CoA synthesis (Table S2). Stringent response induction by mupirocin led to decreases in malonyl-CoA pools (~6-fold) and in P_{accBC}-*lacZ* β-gal activity (~4-fold) (Fig. 1C). Similarly, stationary-phase cells showed ~2-fold lower malonyl-CoA production and P_{accBC}-*lacZ* β-gal activity compared to exponential-phase cells (Fig. 1D). Finally, the P_{accBC}-*lacZ* reporter was inhibited by mupirocin in HG1-R, but not in the ppGpp0 strain (Fig. S2C). These results show that in *S. aureus*, stringent response induction leads to repression of malonyl-CoA synthesis (13).

FASII-antibiotic-induced latency transiently alters expression of (p)ppGpp-regulated sensors. We recently showed that host fatty acids can compensate FASII-antibiotic inhibition of *S. aureus* to promote growth. In low membrane stress conditions, as in serum, adaptation involves a transient latency phase without detection of FASII mutations (Fig. 2A). Anti-FASII-adapted *S. aureus* display fatty acid profiles that are fully exogenous (Fig. S1B) (5). As anti-FASII treatment may provoke fatty acid deprivation before eFAs are incorporated, we asked whether the latency preceding FASII bypass corresponds to stringent response induction. Using the stringent response sensors, an ~3.9-fold increase in P_{ilvD}-*lacZ* and ~7-fold decrease of P_{cshA}-*lacZ* β-gal activities were observed during the latency phase preceding outgrowth (Fig. 2B), indicating that a factor related to the stringent response is induced in response to anti-FASII treatment.

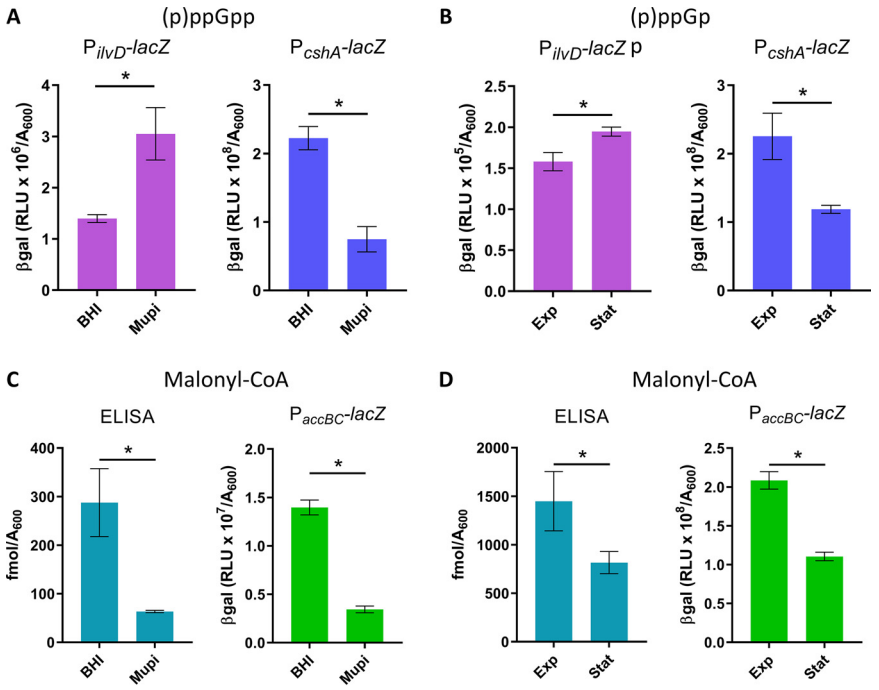

FIG 1 Mupirocin and stationary-phase conditions stimulate (p)ppGpp sensor responses and inhibit malonyl-CoA production and *accBC* activity. *S. aureus* Newman strains contain reporter systems as indicated. Strains were grown in BHI and BHI containing 0.1 μg/ml mupirocin (Mupi) for 1 h (A and C), or in SerFA at exponential (A_{600}~4.0, Exp) and stationary phase (A_{600} ~10.0, Stat) (B and D). P$_{ilvD}$-*lacZ* and P$_{cshA}$-*lacZ* expression were evaluated by β-gal assays. Total malonyl-CoA levels were determined by immunoassay (ELISA) and deduced from P$_{accBC}$-*lacZ* expression. Genes *ilvD* and *cshA* are upregulated and downregulated, respectively, by stringent response induction. Data presented are means ± standard deviations from triplicate independent experiments. *, $P \leq 0.05$ using the Mann-Whitney test.

P$_{ilvD}$-*lacZ* activity returned to normal levels once bacteria were in the outgrowth phase. P$_{cshA}$-*lacZ* β-gal activity was only partially restored during outgrowth, as levels increased by only 2-fold compared to latency. The reason for lower *cshA* expression is unknown, but it is likely that its expression is subject to other layers of regulation.

FASII antibiotic treatment downregulates *accBC* and lowers malonyl-CoA pools. Malonyl-CoA, the ACC product, binds FapR and antagonizes repression, and is also a FabD substrate (Fig. 3A). We assessed malonyl-CoA production in nonselective (SerFA) and anti-FASII-treated (SerFA-Tric) latency and outgrowth in cultures of the Newman strain. Pools of malonyl-CoA were measured by ELISA and by P$_{accBC}$-*lacZ* expression. Both measurements indicated that malonyl-CoA levels were comparable in SerFA and SerFA-Tric-adapted outgrowth cultures, and were markedly lower during SerFA-Tric latency (Fig. 3B). Taken together, these results show that stringent response induction and anti-FASII-induced latency lead to *accBC* inhibition, suggesting that a common element links these responses.

We also assessed pools of malonyl-CoA using a FapR activity sensor called FapR-Trap (Fig. S3A, Table S2). FapR-Trap responded as expected: expression was increased in the absence of repressor (Δ*fapR*), but decreased in stationary-phase wild-type cells when malonyl-CoA levels were low (Fig. S3B). Interestingly, and in sharp contrast to the above results, malonyl-CoA estimations by FapR-Trap were around 10-fold higher during SerFA-Tric outgrowth compared to nonselective SerFA cultures (Fig. 3C; compare panel B). These differences (summarized in Table S3), particularly visible during adaptation outgrowth, indicate that malonyl-CoA distribution in anti-FASII-treated *S. aureus* favors FapR binding over FabD. They suggest that malonyl-CoA pools and their distribution between FapR and FabD may be central determinants in *S. aureus* adaptation to FASII antibiotics.

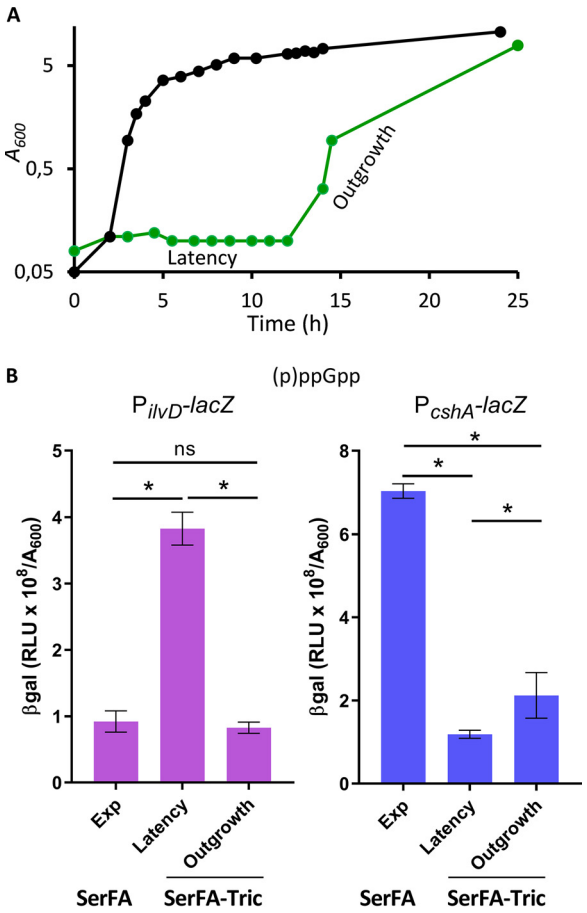

FIG 2 Anti-FASII treatment leads to transient responses of (p)ppGpp sensors. (A) Growth kinetics of *S. aureus* Newman strain in SerFA (black line) and in SerFA-Tric (green line) media. In SerFA-Tric, a 10 to 12 h latency period (Latency) precedes exponential outgrowth (Outgrowth). The growth curves are representative of three independent experiments. BHI and SerFA growth curves are essentially identical; no growth is observed in BHI medium containing triclosan without fatty acids ($n = 3$, not shown). (B) Stringent response status according to growth condition in the Newman strain carrying the P_{ilvD}-*lacZ* reporter (left) and P_{cshA}-*lacZ* (right). β-Gal activities of samples in SerFA (exponential growth [Exp], A_{600} = ~1.5) and SerFA-Tric (Latency, A_{600} = ~0.3) were measured after 3 h of growth. β-Gal activities were measured on 17-h samples in SerFA-Tric (exponential growth [Outgrowth], A_{600} = ~1.5). Data presented are means ± standard deviations from triplicate independent experiments. *, $P \leq 0.05$; ns, not significant, using Mann-Whitney tests.

Reduced FabD competition for malonyl-CoA would increase its availability for FapR (Fig. 3A). We showed previously that *fabD* mutants may emerge upon FASII-antibiotic selection, but not in serum-supplemented medium as used here (4, 5). Indeed, a *fabD* mutant displayed 5-fold greater FapR-Trap expression than the parental strain in non-selective SerFA (Fig. 3D). However, we ruled out the presence of *fabD* mutations in our conditions by sequencing the DNA of five independent anti-FASII-adapted cultures (available upon request). These findings could suggest that FabD is intact but disabled for its interactions with malonyl-CoA during *S. aureus* growth in the presence of anti-FASII. This possibility is currently under study in our laboratory.

GTP depletion is the feature common to the stringent response and FASII-antibiotic-induced latency. We asked whether the stringent response effector (p)ppGpp was directly responsible for the observed phenotypes during anti-FASII treatment, using an *S. aureus* wild type (WT) strain (HG1-R) and the (p)ppGpp0 isogenic strain (called ppGpp0). AFN-1252 was used as anti-FASII in this strain background due to higher resistance of HG001 derivatives to triclosan. The HG1-R and ppGpp0 strains grew similarly in the presence of anti-FASII treatment, suggesting that the absence of (p)ppGpp did not accelerate anti-FASII adaptation (data not shown). We then

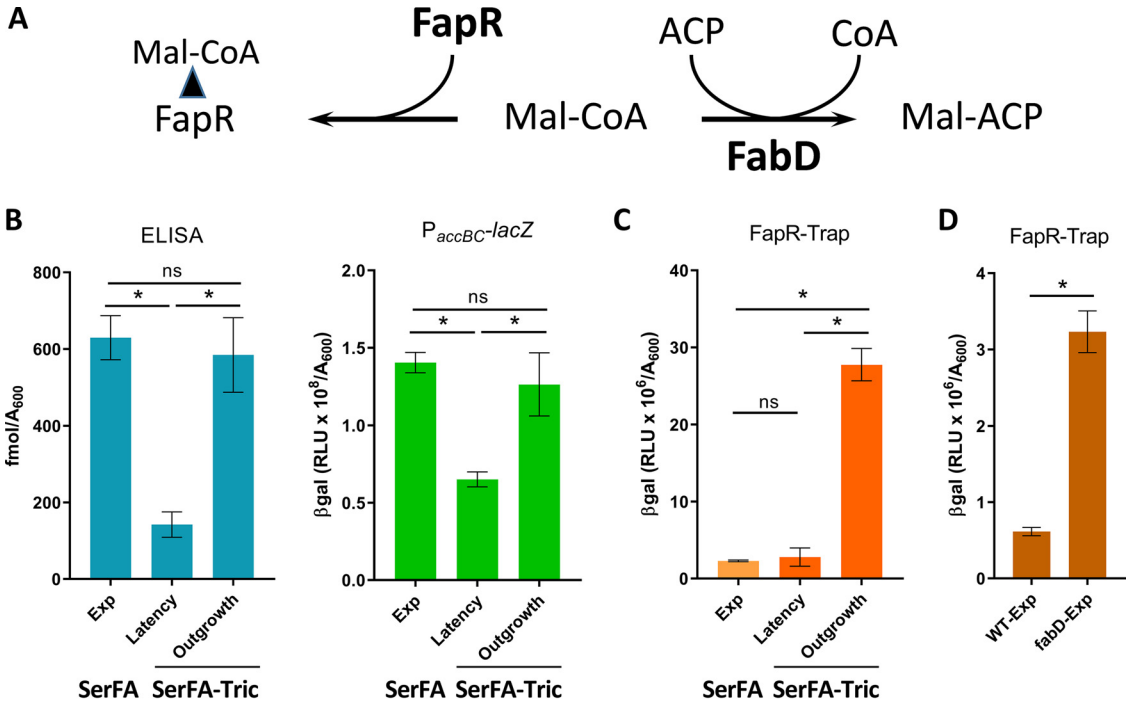

FIG 3 Anti-FASII treatment leads to transient *acc* repression and shifts in malonyl-CoA distribution. (A) Schematic diagram illustrating two known malonyl-CoA interactants, FapR and FabD. FapR is a repressor of FASII and phospholipid synthesis. Malonyl-CoA binds FapR (left), which reverses FapR repressor activity. FabD uses malonyl-CoA to produce malonyl-ACP, the FASII precursor (right). (B) Assessment of malonyl-CoA production by ELISA and P_{accBC}-*lacZ*. Sandwich ELISA was used to measure total malonyl-CoA (left) (see the Materials and Methods for detail) and P_{accBC}-*lacZ* reporter activity (right). (C) Assessment of FapR-bound malonyl-CoA. FASII-antibiotic-adapted *S. aureus* display altered malonyl-CoA distribution (see A). The Newman strain and derivatives were grown in nonselective (SerFA) and anti-FASII (SerFA-Tric) media. β-Gal activities were measured in SerFA at A_{600} = ~2.0 (exponential growth [Exp]) and in SerFA-Tric during latency after 3 h growth (A_{600} = ~0.3 [Latency]) and upon adaptive exponential outgrowth (A_{600} = ~2 [Outgrowth]). (D) Assessment of FapR-bound malonyl-CoA in a *fabD* mutant using FapR-Trap. β-Gal assays of wild-type Newman strain and *fabD* mutant (CondT^R-17, a point mutant [4]) carrying FapR-Trap were performed in SerFA after 3 h growth (A_{600} = ~1.0 [Exp]). Measurements in B to D represent means ± standard deviations from triplicate independent experiments. *, $P \leq 0.05$, ns, not significant, using Mann-Whitney tests.

compared expression of P_{ilvD}-*lacZ* and P_{accBC}-*lacZ* sensors in the WT versus ppGpp0 backgrounds upon anti-FASII treatment (Fig. 4A). Both sensors behaved as described above (Fig. 2 and 3) in the WT strain. However, these sensors displayed the same responses to anti-FASII treatment in the two strains. Thus, while (p)ppGpp induction inhibits *acc* and thus lowers malonyl-CoA pools, it is not required for these phenotypes in anti-FASII-treated *S. aureus*.

(p)ppGpp is known to be intimately linked to GTP, as (p)ppGpp inhibits GTP synthesis (30, 31). Lowering GTP levels rescues *B. subtilis* from ppGpp0 toxicity during lipid starvation (20). We used HPLC to measure GTP levels during anti-FASII adaptation of *S. aureus* Newman. GTP levels decreased by 4-fold at 3 h post-anti-FASII treatment (Fig. 4B). Consistent with this, the amounts of two GTP synthesis enzymes were decreased during anti-FASII latency of *S. aureus* USA300, as seen by proteomics (5); HprT (2.35-fold lower [$n = 4$]; $P = 0.014$) and GuaA (1.5-fold lower [$n = 4$]; $P = 0.029$). These results identify GTP as the metabolite and potential effector common to both the stringent response and anti-FASII-induced latency.

GTP is also a cofactor of the pleiotropic regulator CodY (31). We asked whether CodY is implicated in *accBC* regulation. P_{accBC}-*lacZ* expression was visibly lower in a *codY* insertional mutant compared to expression in the parental WT (USA300) (Fig. 4C). In addition, the anti-FASII latency period was strikingly longer in a *codY* mutant than in the WT strain (Fig. 4D). This delay is consistent with a role of GTP depletion in delaying anti-FASII latency via CodY. These results lead us to propose that, in *S. aureus*, the

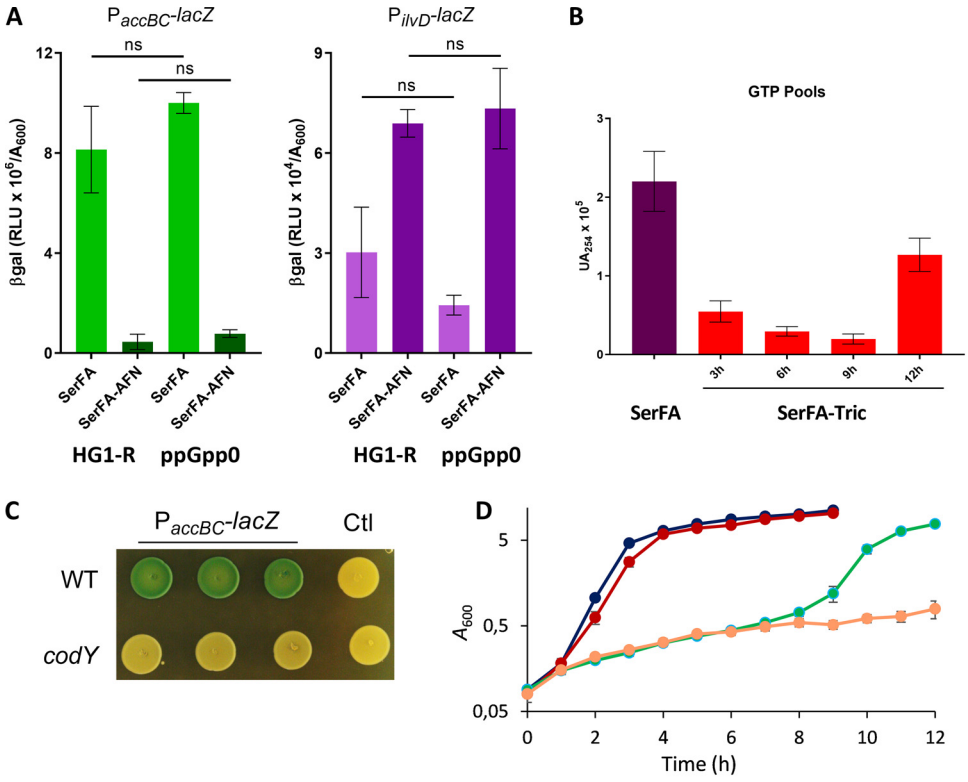

FIG 4 GTP is depleted during anti-FASII latency phase. (A) P_{accBC}-*lacZ* (left) and P_{ilvD}-*lacZ* (right) sensor responses to anti-FASII latency were compared in *S. aureus* HG1-R and the (p)ppGpp null isogenic strain as indicated. β-Gal activities were measured after 3 h of incubation in SerFA and in medium containing the anti-FASII antibiotic AFN-1252. Data presented are means ± standard deviations from three biological replicates. P values were determined pairwise by Mann-Whitney; ns, not significant. (B) Newman strain GTP levels were assessed at different growth times during anti-FASII latency (3 h, 6 h, and 9 h) and outgrowth (12 h). Data presented are means ± standard deviations from duplicate independent experiments. (C) P_{accBC}-*lacZ* expression is lower in a *codY* mutant. USA300 and the *codY* derivative contained plasmids expressing P_{accBC}-*lacZ* or the control plasmid (pTCV-*lac* [Ctl]). Exponential-phase cultures issued from three independent colonies were adjusted to A_{600} = 0.1 and 5-μl drops were plated onto BHI plates containing erythromycin (5 μg/ml) and X-gal. Photographs were taken after 20 h at 37°C and 24 h at 4°C. (D) Growth rates of *S. aureus* USA300 and a confirmed *codY* mutant of the Nebraska mutant collection were compared in nonselective (SerFA) and SerFA-Tric conditions in four independent replicates. Black, WT in SerFA; red, *codY* in SerFA; green, WT in SerFA-Tric; orange, *codY* in SerFA-Tric. Mean and standard deviation are shown for each time point.

stringent response pathway intersects the initial latency response to FASII inhibitors by the common depletion of GTP, likely via the CodY regulon.

Phospholipid synthesis genes *plsX* and *plsC* are differently controlled by FapR. The above results show that malonyl-CoA pools are restored during *S. aureus* adaptation to FASII antibiotics, and preferentially bind FapR, which alleviates FapR repression (Fig. 3). The *S. aureus* FapR regulon reportedly includes *plsX* (NWMN_1139, part of the *fapR* operon) and *plsC* (NWMN_1620); however, the *S. aureus* FapR binding site in the *plsC* promoter region is highly degenerate (13) (see Fig. 5A), and no proof was given for this interaction. We used promoter reporter fusions $P_{fapR\ plsX}$-*lacZ* and P_{plsC}-*lacZ* (Table S2) to compare expression in a wild-type strain (HG1-R) and its Δ*fapR* derivative. Expression of both reporters was upregulated (each 1.6-fold) in the Δ*fapR* strain (Fig. 5B). To determine whether regulation involved direct FapR binding, we performed DNase I footprinting using the *plsX* and *plsC* promoters as binding substrates for purified FapR (Fig. 5C). FapR bound efficiently to the *plsX* promoter region. In contrast, FapR did not bind the *plsC* upstream region containing the putative binding site. Taken together, these results indicate that in *S. aureus*, FapR regulates expression of both *plsX* and *plsC*, but that its effect on *plsC* is either indirect or may require other *S. aureus* factors.

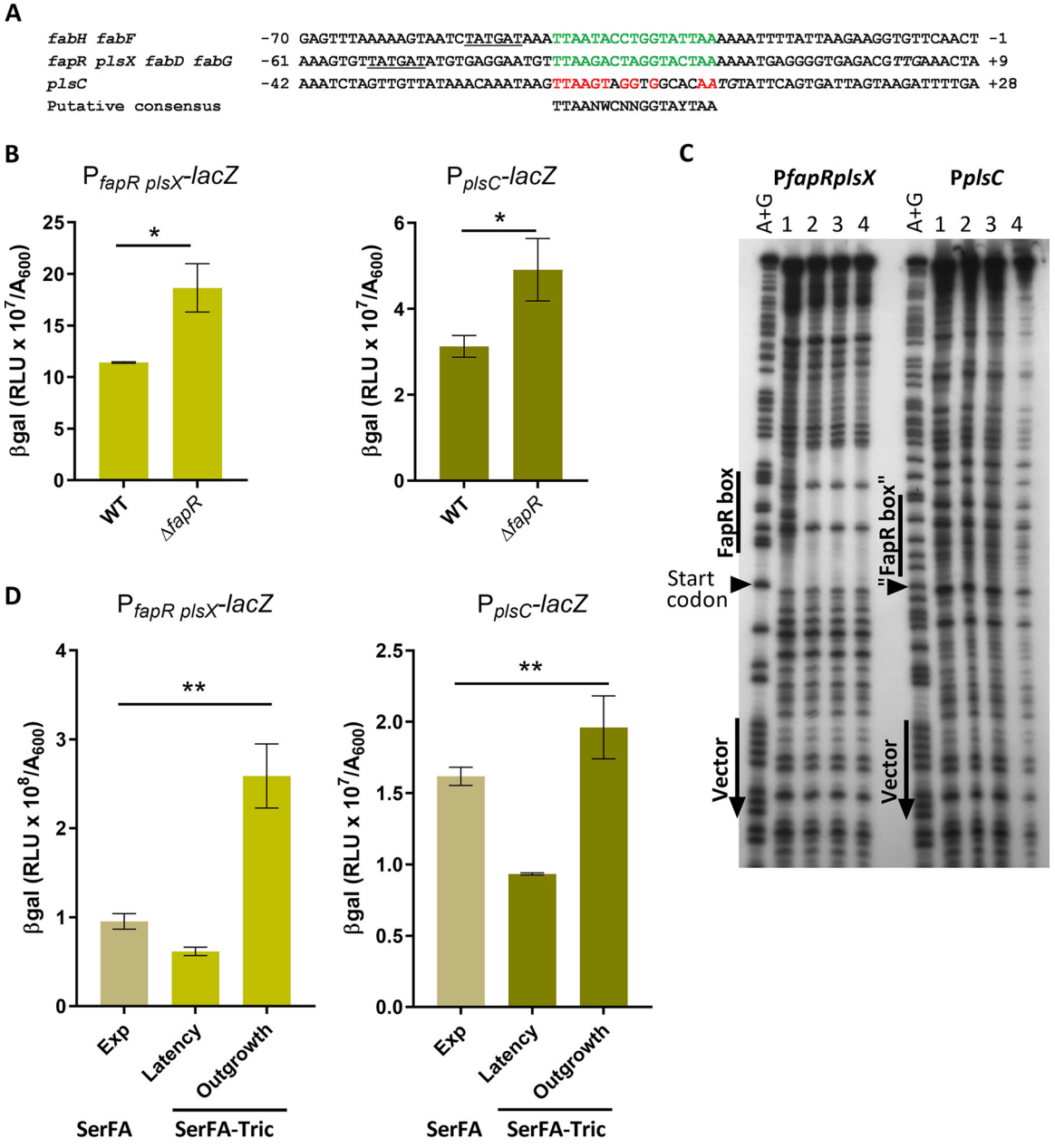

FIG 5 FapR binds the *plsX* but not the *plsC* promoter region, but affects expression of both genes. (A) Sequence alignment of FapR-binding sites in *S. aureus* as published (13). Positions correspond to the predicted start codon of the first open reading frame (ORF) in each operon. Confirmed 17-bp FapR-binding sequences are in green. The presumed conserved FapR-binding nucleotides upstream of the *plsC* start site are in red. In the consensus sequence below the alignment, N indicates any nucleotide; W indicates A or T; Y indicates T or C. The putative −10 RNA polymerase binding sites are underlined (13). The *plsC* ATG and *fapR* TTG start sites are in italics. (B) Expression of $P_{fapR\ plsX}$-*lacZ* and P_{plsC}-*lacZ* fusions is upregulated in the Δ*fapR* strain. Strains were grown to A_{600} = ~1.5 in SerFA medium prior to β-gal determinations. Data presented are means ± standard deviations from three biological replicates; *, $P \leq 0.05$, ns, not significant, using Mann-Whitney. (C) DNase I footprinting assay of the *PfapRplsX* and P*plsC* promoter regions with FapR. Radiolabeled PCR fragments corresponding to P*plsX* and P*plsC* were used as DNA targets. Various amounts of FapR (lane 1, 0 nmol; lane 2, 1.2 nmol; lane 3, 6 nmol; and lane 4, 12 nmol) were incubated with 0.2 pmol DNA before DNase 1 digestion. Lane A+G contains the Maxam and Gilbert reaction of the labeled strand. Positions of vector and "FapR box" sequences are indicated by vertical lines, *plsX* and *plsC* start codons are indicated by black arrows. (D) Expression of $P_{fapR\ plsX}$-*lacZ* and P_{plsC}-*lacZ* fusions in *S. aureus* Newman strain during growth in nonselective (SerFA) and anti-FASII (SerFA-Tric) media. β-Gal values are shown for samples processed in SerFA at optical density at 600 nm (OD_{600}) = ~2.0 (exponential phase [Exp]) and in SerFA-Tric after 3 h in latency (OD_{600} = ~0.3) and upon adaptation outgrowth at 17 h (OD_{600} = ~2.0 [Outgrowth]). Means and standard deviations are shown for three independent experiments. P values were determined by Kruskal-Wallis test; **, $P \leq 0.005$; ns, not significant.

Mupirocin and anti-FASII treatment lead to reduced expression of *S. aureus* phospholipid synthesis genes *plsX* and *plsC*. Repression of *accBC* FASII by mupirocin would be expected to impact all FapR-regulated genes, including those involved in phospholipid synthesis (Fig. S1A). To test this, we followed $P_{fapRplsX}$-*lacZ* and P_{plsC}-*lacZ* transcriptional fusion expression in the presence of mupirocin (0.1 μg/ml), using P_{ilvD}-*lacZ* and P_{accBC}-*lacZ* sensors as references (Table S4). Expression of *plsX* and *plsC* sensor fusions were 4- and 3-fold lower, respectively, in mupirocin than in nontreated samples.

Responses of $P_{fapRplsX}$-*lacZ* and P_{plsC}-*lacZ* during anti-FASII-induced latency and outgrowth were then measured. Expression of β-gal from both sensors gradually decreased during latency, followed by abrupt (4- and 2-fold, respectively) increases upon restart of active growth of anti-FASII-adapted cells (Fig. 5D, and data not shown). Expression of $P_{fapRplsX}$-*lacZ* reached higher (~3-fold) levels in anti-FASII-adapted outgrowth than in nonselective growth. Anti-FASII treatment thus decreases expression of phospholipid synthesis genes during latency, which recovers upon adaptation.

Mupirocin treatment lowers fatty acid incorporation and is synergistic with anti-FASII treatment to inhibit *S. aureus* growth. Since mupirocin leads to downregulation of phospholipid synthesis genes, it might consequently affect *S. aureus* membrane fatty acid composition. To test this, *S. aureus* strain Newman was grown in SerFA with and without sublethal mupirocin addition (0.05 μg/ml, i.e., 5-fold below the MIC) (32). Incorporated eFA was markedly decreased, from 50% in nontreated to 35% in mupirocin-treated cultures (Fig. 6A). Induction of (p)ppGpp during anti-FASII-induced latency could thus slow or stop eFA incorporation in this transient period.

The above findings led us to hypothesize that FASII inhibitors could be synergistic with a stringent response inducer that prevents compensatory eFA incorporation by repressing the phospholipid synthesis genes *plsX* and *plsC*. We first examined anti-FASII adaptation in a strain expressing (p)ppGpp (via *relP*-expressing plasmid pCG258 in a ppGpp0 strain [26]), (Table S2). While the ppGpp0 control strain (carrying the empty vector pCG248) adapted to anti-FASII after overnight growth, basal RelP expression was sufficient to inhibit anti-FASII adaptation (Fig. 6B). This result shows that (p)ppGpp accumulation synergizes with anti-FASII action to block *S. aureus* growth. Likewise, addition of a subinhibitory concentration of mupirocin (0.05 μg/ml) and triclosan (0.5 μg/ml) to *S. aureus* SerFA cultures resulted in extended latency, whereas neither mupirocin nor the anti-FASII treatment separately blocked bacterial growth (Fig. 6C). Similar results were obtained using anti-FASII AFN-1252 (7) and the multidrug-resistant *S. aureus* (MRSA) strain USA300 FPR3757 (Table S5). Thus, the observed synergistic effect between two flawed antibiotics may offer an effective strategy for development of last-resort treatments against *S. aureus* infection.

DISCUSSION

This study reveals the nature of cross-control between *S. aureus* responses to FASII inhibition and to stringent conditions. GTP is depleted in both these conditions, which may explain why the same targets are affected. Our results further show that (p)ppGpp induction lengthens the latency phase preceding adaptation to FASII inhibition. *accBC* transcription is repressed upon stringent response induction, which sets off a chain of events leading to transient repression of the phospholipid synthesis genes *plsX* and *plsC*. These events correlate with limited eFA incorporation and extended latency. During *S. aureus* adaptation outgrowth, the initial effects of anti-FASII are reversed, allowing eFA incorporation and adaptation to FASII antibiotics. These results suggest a model (Fig. 7) in which (p)ppGpp induction and anti-FASII both initially trigger GTP depletion, resulting in decreased malonyl-CoA pools. The suggested role for CodY in regulating ACC expression remains to be investigated. These events repress phospholipid enzyme synthesis and contribute to anti-FASII latency prior to adaptation outgrowth. Stringent conditions in host niches may be relevant to *S. aureus* infection (33), and might impact the bacterial response to anti-FASII treatment. While our findings identify a role for (p)ppGpp induction via GTP depletion in anti-FASII adaptation in *S.*

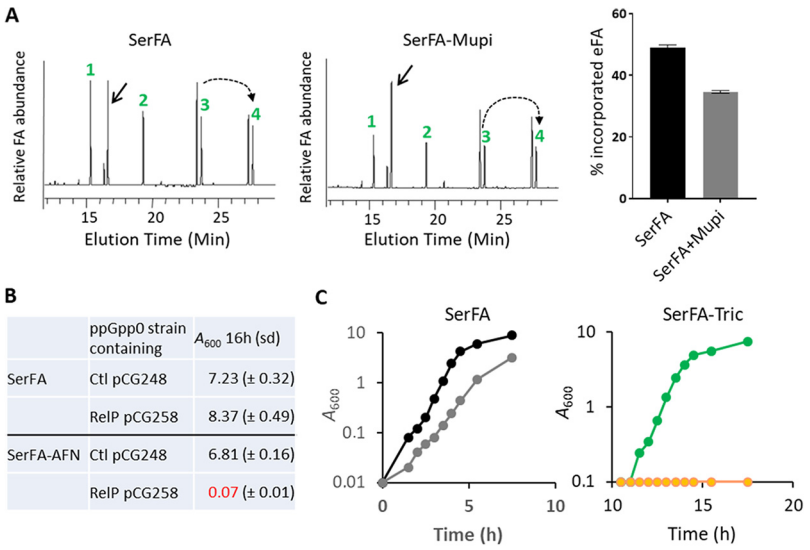

	ppGpp0 strain containing	A_{600} 16h (sd)
SerFA	Ctl pCG248	7.23 (± 0.32)
	RelP pCG258	8.37 (± 0.49)
SerFA-AFN	Ctl pCG248	6.81 (± 0.16)
	RelP pCG258	0.07 (± 0.01)

FIG 6 Subinhibitory mupirocin inhibits *S. aureus* eFA incorporation in membrane phospholipids and synergizes with anti-FASII to inhibit adaptation. (A, left) Fatty acid profiles of *S. aureus* Newman grown in SerFA and SerFA+mupirocin (mupi). Samples were processed after 3 h growth. Black arrow, position of the main endogenous fatty acid *ai*15:0. Fatty acids (eFA) are as follows: 1, C14:0; 2, C16:0; 3, C18:1; and 4, C20:1 (elongation of C18:1). Dashed arrow, elongation of C18:1 ($n + 2$). (A, right) Percent eFA of Newman grown in SerFA without and with mupirocin, derived from integration of two fatty acid profiles from two independent experiments. (B) Control plasmid pCG248 and aTc-inducible *relP*-expressing plasmid pCG258 (26) were established in the ppGpp0 (null) strain. Strains were grown in SerFA and SerFA-AFN for 16 h in the absence of inducer. Anti-FASII adaptation is inhibited in the (p)ppGpp-expressing strain. (C) *S. aureus* Newman was grown in SerFA (black) and SerFA+mupi (gray) (left) or in SerFA-Tric (green) and SerFA-Tric+mupi (orange) (right). Growth was monitored by A_{600}. Growth curves at right are shown starting at 10 h. Mupi was used at 0.05 μg/ml. Results are representative of three independent experiments.

aureus, they do not rule out other roles for these metabolites, or the involvement of other factors in this process.

A new role for malonyl-CoA in anti-FASII adaptation was uncovered in this study, via its increased association with FapR in antibiotic-adapted cultures compared to non-selective cultures. FapR-Trap showed ~10-fold greater expression in anti-FASII-adapted cultures than in nonselective cultures, while total malonyl-CoA pools were the same in both conditions (Fig. 3). Increased malonyl-CoA interaction with FapR, i.e., FapR derepression, during anti-FASII adaptation is consistent with increased *plsX* and *plsC* expression (Fig. 5). Malonyl-CoA rerouting in anti-FASII treatment may be explained by FabD inactivation in anti-FASII adaptation conditions, e.g., by an intermediate metabolite, as suggested in *E. coli* (34). Along this line, a recent study proposed that acyl-ACP accumulation could inhibit FabD (35). Interestingly, acyl-ACP accumulates in a *fabD* mutant during anti-FASII adaptation (4). Alternative possibilities may be considered, such as (i) post-translational FabD modification (36) or (ii) FabD reversal upon FASII inhibition due to a pile-up of its endproduct, malonyl-ACP. We are currently investigating these hypotheses. These findings indicate limits to the reliability of FapR operon-based sensors to estimate malonyl-CoA pools, for which readouts vary according to growth conditions. This may be important to consider in bioengineering applications that rely on FapR operon-like sensors to optimize malonyl-CoA production (37).

Previous studies identified *S. aureus plsC* as containing a FapR-binding site (13). This is disproven here, as FapR failed to bind the published *plsC* consensus site, which lacks a consensus palindromic sequence (Fig. 5C). Nevertheless, *plsC* expression is increased in a Δ*fapR* mutant, indicating that FapR-mediated control is indirect.

The need for antimicrobial alternatives is urgent and, besides the discovery of new molecules or targets, the development of efficient combinations based on existing but

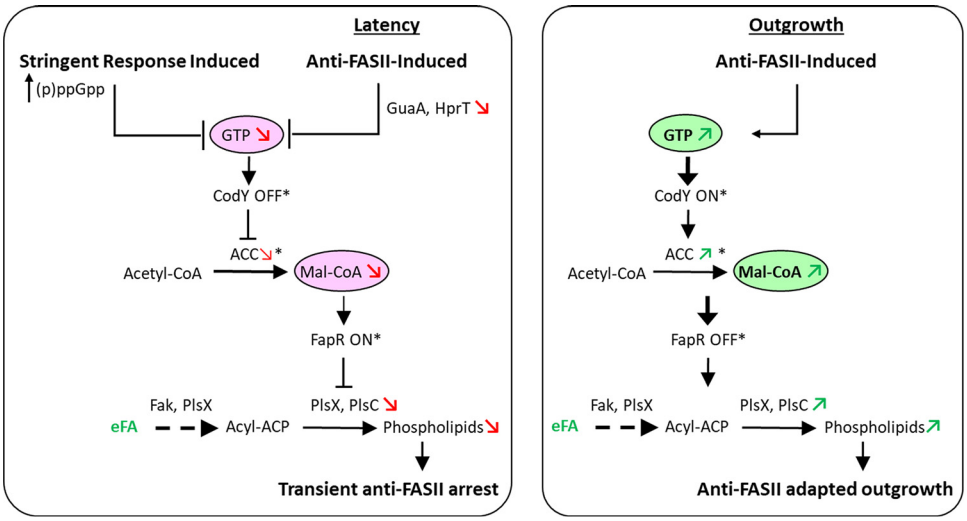

FIG 7 Model for intersecting control of the stringent response and FASII inhibition in *S. aureus*. (Left) Stringent response induction leads to GTP depletion, which in turn modulates gene expression to prepare for starvation (20, 31). We showed that inhibition of FASII also leads to GTP depletion, pointing to an intersecting link between these pathways. Both conditions activate stringent response sensors (P_{ilvD}-*lacZ*, P_{oppB}-*lacZ*, and P_{cshA}-*lacZ*) and lower malonyl-CoA (mal-CoA) pools, such that FapR (for which mal-CoA acts as anti-repressor) exerts repression (13). As a consequence, genes under FapR control, including *plsX* and *plsC*, remain repressed, blocking phospholipid synthesis. Both stringent response induction and FASII inhibition during the latency phase lead to membrane synthesis arrest. (Right) Upon FASII adaptation, GTP levels are restored. *accBC* expression is restored to normal, and mal-CoA levels are increased, leading to FapR derepression. In consequence, PlsX and PlsC are both increased, such that phospholipid synthesis resumes. Red and green arrows and circled metabolites correspond to functions analyzed in this study. * refers to activities based on previous studies.

individually ineffective drugs remains to be explored. Our clarification of the link between the stringent response and anti-FASII adaptation opens perspectives for combinatorial antibiotic strategies, using FASII inhibitory and subinhibitory concentrations of stringent response inducers that delay or prevent anti-FASII adaptation of multidrug resistant pathogens like *S. aureus*. Mupirocin, which is usually used topically, was recently proposed as a potentially active systemic antibiotic when presented in liposomes (38). The proof-of-concept demonstrated here using anti-FASII antibiotics and mupirocin suggests a useful bi-therapy approach for reducing *S. aureus* survival during infection.

MATERIALS AND METHODS

Strains and media. Strains are listed in Table S1 in the supplemental material. Brain heart infusion (BHI) and Luria-Bertani (LB) media were used, respectively, for *S. aureus* and *E.coli* growth. *S. aureus* precultures were routinely prepared in BHI medium. Three fatty acids (C14:0, myristic acid; C16:0, palmitic acid; and C18:1, oleic acid) (Larodan Fine Chemicals, Stockholm, Sweden) were prepared as 100 mM stocks in dimethyl sulfoxide (DMSO) and used at final equimolar concentrations of 0.17 mM each in experiments (referred to as eFA). Ser-FA (BHI containing eFA + 10% newborn calf serum) (Sigma-Aldrich, St. Louis, MO) and SerFA-Tric (SerFA plus triclosan, 0.5 μg/ml), or SerFA-AFN (SerFA plus AFN-1252, 0.5 μg/ml) were the modified media used as indicated. Antibiotics kanamycin (50 μg/ml) and erythromycin (5 μg/ml) were used in *E. coli* and *S. aureus,* respectively, to select pTCV-*lac*-based reporter fusion plasmids (39). Antibiotic adaptation experiments with plasmid-carrying strains were done in SerFA-Tric containing 2 μg/ml erythromycin; note that the latency period was extended by about 4 to 6 h under this condition. Mupirocin (Clinisciences, Nanterre, France), a functional analogue of isoleucyl-AMP and a stringent response inducer of (p)ppGpp (40), was prepared in DMSO and used at 0.1 μg/ml (32, 41) to validate (p)ppGpp sensors, or at 0.05 μg/ml when used in combination with anti-FASII antibiotics. Equal volumes of DMSO were added to control samples when mupirocin was used.

Growth experiments in anti-FASII conditions. Three *S. aureus* strains or their derivatives were used to follow anti-FASII adaptation: Newman, USA300, and HG1-R. The latter strain corresponds to HG001 that was repaired for a *fakB1* defect present in the 8325 lineage, and in a minority of *S. aureus* strains; *fakB1* encodes a fatty acid kinase subunit for saturated fatty acid phosphorylation, which enables the use of eFA during anti-FASII adaptation. The above strains showed comparable responses to conditions tested in this work. In experiments using triclosan as the anti-FASII antibiotic, cells were precultured in BHI and then diluted to absorbance at 600 nm (A_{600}) of 0.01 in SerFA-Tric. Growth was followed by A_{600}

readings as indicated. Nonselective exponential- and stationary-phase cultures were harvested at A_{600}= 1 to 4, and ~10, respectively. If AFN-1252 was used as the anti-FASII antibiotic, the procedure was the same except that precultures were done in SerFA. Both triclosan and AFN-1252 specifically inhibit FabI, a FASII enzyme (7, 42). Triclosan causes nonspecific membrane damage at higher concentrations (42) and was therefore not used in studies with the HG1-R strain, which showed higher resistance to this drug.

Construction of *fakB1*-repaired strains. The *fakB1* gene of *S. aureus* HG001, as the entire 8325 lineage, displays a 483-bp deletion removing 56% of the 867-bp functional gene. To repair this deletion, a 1,939-bp DNA fragment containing a functional *fakB1* was amplified by PCR from *S. aureus* JE2 with primers fakB1_fp and fakB1_rp (Table S6). This fragment was cloned using the Gibson assembly protocol in the thermosensitive vector pG1 (43) amplified with the primers pG1_GibBam and pG1_GibEco (Table S6). The resulting vector pG1Ω*fakB1* was introduced by electroporation into *S. aureus* HG001, HG001Δ*fapR*, and HG001ppGpp0 strains to generate corresponding *fakB1*-repaired strains (Table S1). Electroporation of *S. aureus* strains and allelic exchange were performed as described previously (44). The expected *fakB1* repair in these strains was confirmed by PCR and sequence analysis.

Reporter fusions. Promoter regions of *ilvD*, *oppB*, *cshA*, as well as *fapR*, *plsC*, and *accBC*, were cloned in pTCV-*lac* or pAW8 plasmids (Table S2) using the appropriate primers (Table S6). PCR-amplified DNA fragments and plasmid were treated with restriction enzymes EcoRI and BamHI and ligated products were transformed into DH5α, Top10, or IM08B *E. coli* cells. The obtained constructs were confirmed by DNA sequencing. Plasmids obtained from IM08B were used directly to transform the *S. aureus* Newman strain; clones obtained in DH5α or Top10 were first established in the *S. aureus* strain RN4220. A standard electroporation protocol was used to transform DNA in *S. aureus* (45).

(p)ppGpp sensors. The genes *ilvD* (NWMN_1960) and *oppB* (NWMN_0856) are upregulated, while the *cshA* (NWMN_1985) gene is downregulated, upon stringent response induction (24, 40, 46). The corresponding stringent response sensors P_{ilvD}-*lacZ*, P_{oppB}-*lacZ*, and P_{cshA}-*lacZ* (Table S2) were tested in medium containing 0.1 μg/ml mupirocin (40), and validated as *bona fide* (p)ppGpp sensors (Fig. 1A).

FapR activity sensor. To estimate malonyl-CoA pools bound to FapR, we designed a transcriptional fusion with promoter and operator sequences containing a consensus FapR-binding site and called it FapR-Trap (Fig. S2, Table S2). The construction was based on similar previous studies to estimate malonyl-CoA pools (37, 47).

β-Galactosidase assays. Fresh cultures were prepared at A_{600} = 0.1 from overnight BHI cultures and β-galactosidase (β-gal) activities were measured at the indicated A_{600} or time of sampling. When mupirocin was used, cultures were treated or not at A_{600} = 0.1 after growth from an initial A_{600} = 0.01 and processed 1 h later. All samples of a set were stored at −20°C prior to measurements, which were performed for all samples of a same set. β-Gal activities were measured as described previously (48), except that samples derived from SerFA-containing medium were incubated with lysostaphin (0.1 mg/ml; AMBI Products, Tarrytown, NY) for 30 min at room temperature prior to processing with β-Glo reagents (Promega Co., Madison, WI). The values of β-gal (mean ± standard deviation) were determined from three independently performed experiments.

Malonyl-CoA measurement by ELISA. Bacterial cultures were prepared as described above, and samples were processed at the indicated A_{600}/time interval according to our test conditions. For each sample, the equivalent of A_{600} = 30 was centrifuged at 8,000 rpm at room temperature for 5 min. Pelleted cells were immediately frozen in liquid nitrogen and transferred to –80°C overnight. Ice-cold phosphate-buffered saline (PBS) was used to resuspend cells at 4°C, which were then sonicated in FastPrep (MP Biomedical, Solon, OH). Supernatants were collected by centrifuging the cell slurry at 13,000 rpm at 4°C for 5 min, and stored at –80°C until use. ELISAs for total malonyl-CoA measurements were performed as per the manufacturer's instructions (CUSABIO Life Sciences, College Park, MD). Malonyl-CoA standards were run along with test samples. Each experiment was performed on three independent cultures. Mean values ± standard deviation are presented.

For malonyl-CoA measurements under stringent response conditions (Fig. 1C, left), the Newman strain was first grown in BHI to an A_{600} of 0.5 from an initial inoculum of 0.01. Cultures were treated or not with 0.1 μg/ml mupirocin for 30 min (A_{600} = ~1 for both samples). ELISAs were performed as described above.

Purification of *S. aureus* FapR. The*S. aureus fapR* gene was amplified by PCR with FapRORFfp and FapRORFrp primers (Table S6) and cloned into pET-21b to produce a recombinant FapR carrying an N-terminal His tag and tobacco etch virus (TEV) site expressed in *E. coli* BL21/pDIA17 cells (13, 49). Bacterial cultures were grown at 37°C in LB containing ampicillin (100 μg/ml) and chloramphenicol (10 μg/ml) until A_{600} = 0.6; expression was then induced following addition of IPTG (isopropyl-β-D-thiogalactopyranoside; 0.5 mM) at 20°C for 17 h. Bacteria were harvested by centrifugation (5 g wet weight), washed twice in PBS, and resuspended in 30 ml of buffer A (50 mM Tris-HCl [pH 7.5], 300 mM NaCl, 1 mM dithiothreitol [DTT]), benzonase nuclease (Sigma-Aldrich, St. Louis, MO), and a protease inhibitor cocktail (Roche, Basel, Switzerland). Bacteria were lysed by passage through a CF cell-disrupter (Constant Systems Ltd., Cambridge, United Kingdom) at 4°C. The lysed culture was centrifuged at 46,000 × *g* for 1 h and the supernatant was loaded onto a 1-ml Protino Ni-NTA column (Macherey-Nagel, Diiren, Germany). The protein was eluted with buffer A + 300 mM imidazole and protein-containing fractions were pooled and dialyzed overnight in buffer A with TEV protease (1/10 wt/wt ratio) at 4°C (produced by the Pasteur Institute Production and Purification of Recombinant Proteins Technological Platform). The His-tag-free protein was loaded onto a 1-ml Ni-NTA column and collected. FapR was further purified using a HiLoad 16/60 Superdex 75 prep grade column (GE Healthcare, Madison, WI) equilibrated with 20 mM Tris (pH 7.5), 50 mM NaCl. The purified protein was concentrated and stored at −80°C.

DNase I footprinting. $P_{fapRplsX}$ and P_{plsC} promoter probes were amplified by PCR from pJJ013 ($P_{fapR\ plsX}$-*lacZ*) and pJJ019 (P_{plsC}-*lacZ*) (Table S2), respectively, with specific promoter primers (P*fapRplsX*_Fw; P*plsC*_fd) and vector primer (pTCV-*lac*_rev).

The 5′ end of pTCV-*lac*_Rev was labeled with [γ-^{32}P]ATP using T4 polynucleotide kinase. Before the DNA binding reaction, purified FapR was dialyzed in 100 mM Na_2HPO_4/NaH_2PO_4 (pH 8.0), 250 mM NaCl, 10 mM $MgCl_2$, 5 mM DTT , and 50% glycerol. DNase I footprinting reactions were performed as described previously (50). Briefly, 0 to 12 nmol FapR was mixed with 0.2 pmol of DNA and incubated with DNase 1 at room temperature (~24°C) for 1 min. Samples were analyzed by electrophoresis on a 6% polyacrylamide gel containing 7 M urea. Maxam-Gilbert sequencing ladders (G+A) were loaded on the same gel.

Determination of *S. aureus* fatty acid profiles. Fatty acid profiles were performed as described previously (4). Newman strain precultures prepared from two independent colonies were diluted to A_{600} = 0.1 in SerFA and grown 3 h with and without mupirocin (0.05 μg/ml). A_{600} values of SerFA samples were ~2.5 and treated samples were ~1.0. Percentages of eFA are shown (mean ± standard deviation).

GTP determinations. All extraction steps were performed on ice. Cellular pellets were deproteinized with an equal volume of 6% perchloric acid (PCA), vortex mixed for 20 s, ice bathed for 10 min, and vortex mixed again for 20 s. Acid cell extracts were centrifuged at 13,000 rpm for 10 min at 4°C. The resulting supernatants were supplemented with an equal volume of bi-distilled water, vortex mixed for 60 s, and neutralized by addition of 2 M Na_2CO_3. Extracts were injected onto a C_{18} Supelco 5 μm (250 × 4.6 mm) column (Sigma-Aldrich, St. Louis, MO) at 45°C. The mobile phase was delivered at a flow rate of 1 ml/min using the following stepwise gradient elution program: A to B (60:40) at 0 min→(40:60) at 30 min→(40:60) at 60 min. Buffer A contained 10 mM tetrabutylammonium hydroxide, 10 mM KH_2PO_4, and 0.25% MeOH, and was adjusted to pH 6.9 with 1 M HCl. Buffer B consisted of 5.6 mM tetrabutylammonium hydroxide, 50 mM KH_2PO_4, and 30% MeOH, and was neutralized to pH 7.0 with 1 M NaOH. Detection was done with a diode array detector (PDA). The LC solution workstation chromatography manager was used to pilot the HPLC instrument and to process the data. Products were monitored spectrophotometrically at 254 nm and quantified by integration of the peak absorbance area, employing a calibration curve established with various known nucleosides. Finally, a correction coefficient was applied to correct raw data for minor differences in the total number of cells determined in each culture condition (by A_{600} measurements).

Statistical analyses. Graphs and statistical analyses were prepared using GraphPad Prism software. Means and standard deviations are presented for sensor fusions, ELISA readouts, fatty acid profile comparisons, and GTP measurements. Statistical significance was determined by unpaired, nonparametric Mann-Whitney tests, as recommended for small sample sizes (here biological triplicates) and by a nonparametric, unpaired Kruskal-Wallis test for three-way comparisons.

SUPPLEMENTAL MATERIAL

Supplemental material is available online only.

FIG S1, DOCX file, 0.2 MB.

FIG S2, DOCX file, 1.1 MB.

FIG S3, DOCX file, 0.1 MB.

TABLE S1, DOCX file, 0.029 MB.

TABLE S2, DOCX file, 0.03 MB.

TABLE S3, DOCX file, 0.01 MB.

TABLE S4, DOCX file, 0.01 MB.

TABLE S5, DOCX file, 0.01 MB.

TABLE S6, DOCX file, 0.01 MB.

ACKNOWLEDGMENTS

We acknowledge the valuable comments of anonymous reviewers. We are thankful to Jong-In Hong, Seoul National University, South Korea, for the generous gift of PyDPA used in initial studies. C. Thomas and members of the Institut Pasteur Production and Purification of Recombinant Proteins Platform are gratefully acknowledged for providing purified FapR. Our colleagues P. Bouloc (I2BC, France), C. Morvan (Univ. Paris-Descartes, France), and MicrobAdapt team members E. Borezée-Durant, D. Lechardeur, G. Kénanian, R. Boudjemaa, and P. Gaudu gave valuable advice. G. Dubey and N. Descoeudres provided kind support.

We acknowledge financial support from DIM Malinf (Domaine d'Intérêt Majeur, Maladies Infectieuses) from the Conseil Régional d'Ile-de-France (AP fellowship), French Agence Nationale de la Recherche (StaphEscape project ANR-13001038), Fondation pour la Recherche Medicale (DBF20161136769), and the French Investissement d'Avenir program, Laboratoire d'Excellence Integrative Biology of Emerging Infectious Diseases (grant no. ANR-10-LABX-62-IBEID).

This work is dedicated to our friend and colleague G. Lamberet, who passed away 23 December 2019.

Physiology, molecular biology, (p)ppGpp, GTP, and malonyl-CoA estimation: A.P., M.G., L.D., J.D., D.H., and P.T.-C. Fatty acid analyses: G.L., K.G., and A.G. Data analyses: A.P., J.A.-M., P.T.-C., and A.G. Statistical analysis: D.H. Experimental design and project conception: A.P., P.T.-C., and A.G. A.G. directed the project and A.P., K.G., and A.G. wrote the manuscript.

We declare no competing interests.

REFERENCES

1. Uchil RR, Kohli GS, Katekhaye VM, Swami OC. 2014. Strategies to combat antimicrobial resistance. J Clin Diagn Res 8:ME01–4. https://doi.org/10.7860/JCDR/2014/8925.4529.
2. Lu H, Tonge PJ. 2008. Inhibitors of FabI, an enzyme drug target in the bacterial fatty acid biosynthesis pathway. Acc Chem Res 41:11–20. https://doi.org/10.1021/ar700156e.
3. Brinster S, Lamberet G, Staels B, Trieu-Cuot P, Gruss A, Poyart C. 2009. Type II fatty acid synthesis is not a suitable antibiotic target for Gram-positive pathogens. Nature 458:83–86. https://doi.org/10.1038/nature07772.
4. Morvan C, Halpern D, Kenanian G, Hays C, Anba-Mondoloni J, Brinster S, Kennedy S, Trieu-Cuot P, Poyart C, Lamberet G, Gloux K, Gruss A. 2016. Environmental fatty acids enable emergence of infectious *Staphylococcus aureus* resistant to FASII-targeted antimicrobials. Nat Commun 7:12944. https://doi.org/10.1038/ncomms12944.
5. Kenanian G, Morvan C, Weckel A, Pathania A, Anba-Mondoloni J, Halpern D, Gaillard M, Solgadi A, Dupont L, Henry C, Poyart C, Fouet A, Lamberet G, Gloux K, Gruss A. 2019. Permissive fatty acid incorporation promotes staphylococcal adaptation to FASII antibiotics in host environments. Cell Rep 29:3974–3982. https://doi.org/10.1016/j.celrep.2019.11.071.
6. Wang J, Soisson SM, Young K, Shoop W, Kodali S, Galgoci A, Painter R, Parthasarathy G, Tang YS, Cummings R, Ha S, Dorso K, Motyl M, Jayasuriya H, Ondeyka J, Herath K, Zhang C, Hernandez L, Allocco J, Basilio A, Tormo JR, Genilloud O, Vicente F, Pelaez F, Colwell L, Lee SH, Michael B, Felcetto T, Gill C, Silver LL, Hermes JD, Bartizal K, Barrett J, Schmatz D, Becker JW, Cully D, Singh SB. 2006. Platensimycin is a selective FabF inhibitor with potent antibiotic properties. Nature 441:358–361. https://doi.org/10.1038/nature04784.
7. Banevicius MA, Kaplan N, Hafkin B, Nicolau DP. 2013. Pharmacokinetics, pharmacodynamics and efficacy of novel FabI inhibitor AFN-1252 against MSSA and MRSA in the murine thigh infection model. J Chemother 25:26–31. https://doi.org/10.1179/1973947812Y.0000000061.
8. Escaich S, Prouvensier L, Saccomani M, Durant L, Oxoby M, Gerusz V, Moreau F, Vongsouthi V, Maher K, Morrissey I, Soulama-Mouze C. 2011. The MUT056399 inhibitor of FabI is a new antistaphylococcal compound. Antimicrob Agents Chemother 55:4692–4697. https://doi.org/10.1128/AAC.01248-10.
9. Feng Z, Chakraborty D, Dewell SB, Reddy BV, Brady SF. 2012. Environmental DNA-encoded antibiotics fasamycins A and B inhibit FabF in type II fatty acid biosynthesis. J Am Chem Soc 134:2981–2987. https://doi.org/10.1021/ja207662w.
10. Pishchany G, Mevers E, Ndousse-Fetter S, Horvath DJ, Jr, Paludo CR, Silva-Junior EA, Koren S, Skaar EP, Clardy J, Kolter R. 2018. Amycomicin is a potent and specific antibiotic discovered with a targeted interaction screen. Proc Natl Acad Sci U S A 115:10124–10129. https://doi.org/10.1073/pnas.1807613115.
11. Parsons JB, Frank MW, Subramanian C, Saenkham P, Rock CO. 2011. Metabolic basis for the differential susceptibility of Gram-positive pathogens to fatty acid synthesis inhibitors.Proc Natl Acad Sci U S A 108:15378–15383. https://doi.org/10.1073/pnas.1109208108.
12. Gloux K, Guillemet M, Soler C, Morvan C, Halpern D, Pourcel C, Vu Thien H, Lamberet G, Gruss A. 2017. Clinical relevance of type II fatty acid synthesis bypass in *Staphylococcus aureus*. Antimicrob Agents Chemother 61:e02515-16. https://doi.org/10.1128/AAC.02515-16.
13. Albanesi D, Reh G, Guerin ME, Schaeffer F, Debarbouille M, Buschiazzo A, Schujman GE, de Mendoza D, Alzari PM. 2013. Structural basis for feed-forward transcriptional regulation of membrane lipid homeostasis in *Staphylococcus aureus*.PLoS Pathog 9:e1003108. https://doi.org/10.1371/journal.ppat.1003108.
14. Albanesi D, de Mendoza D. 2016. FapR: from control of membrane lipid homeostasis to a biotechnological tool. Front Mol Biosci 3:64. https://doi.org/10.3389/fmolb.2016.00064.
15. Ruch FE, Vagelos PR. 1973. The isolation and general properties of *Escherichia coli* malonyl coenzyme A-acyl carrier protein transacylase.J Biol Chem 248:8086–8094.
16. Nazir A, Harinarayanan R. 2016. (p)ppGpp and the bacterial cell cycle. J Biosci 41:277–282. https://doi.org/10.1007/s12038-016-9611-3.
17. Potrykus K, Cashel M. 2008. (p)ppGpp: still magical? Annu Rev Microbiol 62:35–51. https://doi.org/10.1146/annurev.micro.62.081307.162903.
18. My L, Rekoske B, Lemke JJ, Viala JP, Gourse RL, Bouveret E. 2013. Transcription of the *Escherichia coli* fatty acid synthesis operon *fabHDG* is directly activated by FadR and inhibited by ppGpp. J Bacteriol 195:3784–3795. https://doi.org/10.1128/JB.00384-13.
19. Janßen HJ, Steinbüchel. 2014. Fatty acid synthesis in *Escherichia coli* and its applications towards the production of fatty acid based biofuels. Biotechnol Biofuels 7:7. https://doi.org/10.1186/1754-6834-7-7.
20. Pulschen AA, Sastre DE, Machinandiarena F, Crotta Asis A, Albanesi D, de Mendoza D, Gueiros-Filho FJ. 2017. The stringent response plays a key role in Bacillus subtilis survival of fatty acid starvation. Mol Microbiol 103:698–712. https://doi.org/10.1111/mmi.13582.
21. Vadia S, Tse JL, Lucena R, Yang Z, Kellogg DR, Wang JD, Levin PA. 2017. Fatty acid availability sets cell envelope capacity and dictates microbial cell size. Curr Biol 27:1757–1767. https://doi.org/10.1016/j.cub.2017.05.076.
22. Greenwood RC, Gentry DR. 2002. The effect of antibiotic treatment on the intracellular nucleotide pools of *Staphylococcus aureus*. FEMS Microbiol Lett 208:203–206. https://doi.org/10.1111/j.1574-6968.2002.tb11082.x.
23. Rhee HW, Lee CR, Cho SH, Song MR, Cashel M, Choy HE, Seok YJ, Hong JI. 2008. Selective fluorescent chemosensor for the bacterial alarmone (p)ppGpp. J Am Chem Soc 130:784–785. https://doi.org/10.1021/ja0759139.
24. Geiger T, Francois P, Liebeke M, Fraunholz M, Goerke C, Krismer B, Schrenzel J, Lalk M, Wolz C. 2012. The stringent response of *Staphylococcus aureus* and its impact on survival after phagocytosis through the induction of intracellular PSMs expression.PLoS Pathog 8:e1003016. https://doi.org/10.1371/journal.ppat.1003016.
25. Herbert S, Ziebandt AK, Ohlsen K, Schafer T, Hecker M, Albrecht D, Novick R, Gotz F. 2010. Repair of global regulators in *Staphylococcus aureus* 8325 and comparative analysis with other clinical isolates. Infect Immun 78:2877–2889. https://doi.org/10.1128/IAI.00088-10.
26. Geiger T, Kastle B, Gratani FL, Goerke C, Wolz C. 2014. Two small (p)ppGpp synthases in *Staphylococcus aureus* mediate tolerance against cell envelope stress conditions. J Bacteriol 196:894–902. https://doi.org/10.1128/JB.01201-13.
27. Parsons JB, Broussard TC, Bose JL, Rosch JW, Jackson P, Subramanian C, Rock CO. 2014. Identification of a two-component fatty acid kinase responsible for host fatty acid incorporation by *Staphylococcus aureus*.Proc Natl Acad Sci U S A 111:10532–10537. https://doi.org/10.1073/pnas.1408797111.
28. Parsons JB, Frank MW, Rosch JW, Rock CO. 2013. *Staphylococcus aureus* fatty acid auxotrophs do not proliferate in mice. Antimicrob Agents Chemother 57:5729–5732. https://doi.org/10.1128/AAC.01038-13.
29. Polakis SE, Guchhait RB, Lane MD. 1973. Stringent control of fatty acid synthesis in *Escherichia coli*. Possible regulation of acetyl coenzyme A carboxylase by ppGpp.J Biol Chem 248:7957–7966.
30. Kriel A, Bittner AN, Kim SH, Liu K, Tehranchi AK, Zou WY, Rendon S, Chen R, Tu BP, Wang JD. 2012. Direct regulation of GTP homeostasis by (p)ppGpp: a critical component of viability and stress resistance. Mol Cell 48:231–241. https://doi.org/10.1016/j.molcel.2012.08.009.
31. Geiger T, Wolz C. 2014. Intersection of the stringent response and the CodY regulon in low GC Gram-positive bacteria.Int J Med Microbiol 304:150–155. https://doi.org/10.1016/j.ijmm.2013.11.013.
32. Rajamuthiah R, Jayamani E, Conery AL, Fuchs BB, Kim W, Johnston T, Vilcinskas A, Ausubel FM, Mylonakis E. 2015. A defensin from the model beetle Tribolium castaneum acts synergistically with telavancin and daptomycin against multidrug resistant *Staphylococcus aureus*. PLoS One 10:e0128576. https://doi.org/10.1371/journal.pone.0128576.

33. Gao W, Chua K, Davies JK, Newton HJ, Seemann T, Harrison PF, Holmes NE, Rhee HW, Hong JI, Hartland EL, Stinear TP, Howden BP. 2010. Two novel point mutations in clinical *Staphylococcus aureus* reduce linezolid susceptibility and switch on the stringent response to promote persistent infection. PLoS Pathog 6:e1000944. https://doi.org/10.1371/journal.ppat.1000944.
34. Kizer L, Pitera DJ, Pfleger BF, Keasling JD. 2008. Application of functional genomics to pathway optimization for increased isoprenoid production. Appl Environ Microbiol 74:3229–3241. https://doi.org/10.1128/AEM.02750-07.
35. Machinandiarena F, Nakamatsu L, Schujman GE, de Mendoza D, Albanesi D. 2020. Revisiting the coupling of fatty acid to phospholipid synthesis in bacteria with FapR regulation.Mol Microbiol 114:653–663. https://doi.org/10.1111/mmi.14574.
36. Kumari R, Saxena R, Tiwari S, Tripathi DK, Srivastava KK. 2013. Rv3080c regulates the rate of inhibition of mycobacteria by isoniazid through FabD. Mol Cell Biochem 374:149–155. https://doi.org/10.1007/s11010-012-1514-5.
37. Johnson AO, Gonzalez-Villanueva M, Wong L, Steinbuchel A, Tee KL, Xu P, Wong TS. 2017. Design and application of genetically-encoded malonyl-CoA biosensors for metabolic engineering of microbial cell factories. Metab Eng 44:253–264. https://doi.org/10.1016/j.ymben.2017.10.011.
38. Goldmann O, Cern A, Musken M, Rohde M, Weiss W, Barenholz Y, Medina E. 2019. Liposomal mupirocin holds promise for systemic treatment of invasive *Staphylococcus aureus* infections. J Control Release 316:292–301. https://doi.org/10.1016/j.jconrel.2019.11.007.
39. Poyart C, Trieu-Cuot P. 1997. A broad-host-range mobilizable shuttle vector for the construction of transcriptional fusions to beta-galactosidase in gram-positive bacteria.FEMS Microbiol Lett 156:193–198. https://doi.org/10.1111/j.1574-6968.1997.tb12726.x.
40. Reiss S, Pane-Farre J, Fuchs S, Francois P, Liebeke M, Schrenzel J, Lindequist U, Lalk M, Wolz C, Hecker M, Engelmann S. 2012. Global analysis of the *Staphylococcus aureus* response to mupirocin.Antimicrob Agents Chemother 56:787–804. https://doi.org/10.1128/AAC.05363-11.
41. Fernandez C, Gaspar C, Torrellas A, Vindel A, Saez-Nieto JA, Cruzet F, Aguilar L. 1995. A double-blind, randomized, placebo-controlled clinical trial to evaluate the safety and efficacy of mupirocin calcium ointment for eliminating nasal carriage of *Staphylococcus aureus* among hospital personnel.J Antimicrob Chemother 35:399–408. https://doi.org/10.1093/jac/35.3.399.
42. McMurry LM, Oethinger M, Levy SB. 1998. Triclosan targets lipid synthesis. Nature 394:531–532. https://doi.org/10.1038/28970.
43. Mistou MY, Dramsi S, Brega S, Poyart C, Trieu-Cuot P. 2009. Molecular dissection of the secA2 locus of group B Streptococcus reveals that glycosylation of the Srr1 LPXTG protein is required for full virulence. J Bacteriol 191:4195–4206. https://doi.org/10.1128/JB.01673-08.
44. Biswas I, Gruss A, Ehrlich SD, Maguin E. 1993. High-efficiency gene inactivation and replacement system for gram-positive bacteria.J Bacteriol 175:3628–3635. https://doi.org/10.1128/jb.175.11.3628-3635.1993.
45. Kraemer GRK, Iandolo JJ. 1990. High-frequency transformation of *Staphylococcus aureus* by electroporation. Curr Microbiol 21:373–376. https://doi.org/10.1007/BF02199440.
46. Anderson KL, Roberts C, Disz T, Vonstein V, Hwang K, Overbeek R, Olson PD, Projan SJ, Dunman PM. 2006. Characterization of the *Staphylococcus aureus* heat shock, cold shock, stringent, and SOS responses and their effects on log-phase mRNA turnover.J Bacteriol 188:6739–6756. https://doi.org/10.1128/JB.00609-06.
47. Ellis JM, Wolfgang MJ. 2012. A genetically encoded metabolite sensor for malonyl-CoA. Chem Biol 19:1333–1339. https://doi.org/10.1016/j.chembiol.2012.08.018.
48. Lechardeur D, Cesselin B, Liebl U, Vos MH, Fernandez A, Brun C, Gruss A, Gaudu P. 2012. Discovery of intracellular heme-binding protein HrtR, which controls heme efflux by the conserved HrtB-HrtA transporter in *Lactococcus lactis*. J Biol Chem 287:4752–4758. https://doi.org/10.1074/jbc.M111.297531.
49. Munier H, Gilles AM, Glaser P, Krin E, Danchin A, Sarfati R, Barzu O. 1991. Isolation and characterization of catalytic and calmodulin-binding domains of *Bordetella pertussis* adenylate cyclase. Eur J Biochem 196:469–474. https://doi.org/10.1111/j.1432-1033.1991.tb15838.x.
50. Derre I, Rapoport G, Msadek T. 1999. CtsR, a novel regulator of stress and heat shock response, controls clp and molecular chaperone gene expression in gram-positive bacteria. Mol Microbiol 31:117–131. https://doi.org/10.1046/j.1365-2958.1999.01152.x.